


Impacts of current and climate induced changes in atmospheric stagnation on Indian surface PM_{2.5} pollution

Received: 4 March 2024

Accepted: 8 August 2024

Published online: 28 August 2024

 Check for updates

Mi Zhou¹✉, Yuanyu Xie¹, Chenggong Wang², Lu Shen³ & Denise L. Mauzerall^{1,4}✉

Severe PM_{2.5} pollution threatens public health in India. Atmospheric stagnation traps emitted pollutants, worsening their health impacts. Global warming is anticipated to alter future stagnation patterns, impacting the effectiveness of air quality policies. Here, we develop a region-specific index that characterizes meteorological conditions driving stagnation and associated PM_{2.5} increases. Applying this index to an ensemble of climate models and global warming scenarios, we find that future stagnation changes result from both global CO₂-driven circulation changes and local aerosol-driven meteorological responses. By 2100, we project an increase in winter stagnation in the Indo-Gangetic Plain (IGP) of 7 ± 3 days that leads to an increase in PM_{2.5} of ~7 ug/m³ in a high-warming and high-aerosol scenario. However, annual stagnation occurrences decrease across most of India. Thus, stringent air quality regulations in the IGP during winters will be critical to reduce surface PM_{2.5} concentrations as climate warms. Such regulations will directly improve air quality while reducing future stagnation occurrences, providing additional air quality benefits.

Elevated fine particulate matter (PM_{2.5}) concentrations have severe adverse health impacts^{1–3}. India experiences some of the highest ambient PM_{2.5} levels in the world, which led to 1.67 million premature deaths in 2019^{4–6}. Extensive efforts to improve air quality over India are underway, targeting major emission sources including residential fuel use, vehicle exhaust, industry, and power generation^{7,8}. These anthropogenic emissions are widely recognized as major causes of hazardous air quality and associated mortality across India^{9–12}. However, other factors, such as meteorological conditions, also play a crucial role⁸.

Meteorological conditions regulate the accumulation, transport, and removal of emitted air pollutants. In conjunction with emissions, they drive observed PM_{2.5} variability on hourly to interannual scales^{13–16}. Atmospheric stagnation, characterized by a lack of precipitation, weak surface winds, and limited vertical mixing, is

particularly influential in driving the buildup of pollution near the surface^{17–20}. Stagnation events can therefore exacerbate PM_{2.5} pollution, even without abrupt emission increases^{21–23}. Recognizing the significant impact of stagnation on air quality, researchers have developed several region-specific indices to accurately identify their occurrence over the United States (US), Europe, and China^{22,24–26}. These indices rely on meteorological factors that are either well correlated with surface particulate matter concentrations or indicative of atmospheric dispersion strength in these locations. They are effective in identifying elevated particulate matter episodes over the regions for which they have been developed^{14,21–23}. However, no India specific index has previously been developed.

Climate change is projected to alter atmospheric circulation and precipitation patterns, subsequently influencing the occurrence of weather patterns that worsen air quality^{13,27,28}. However, in India,

¹Princeton School of Public and International Affairs, Princeton University, Princeton, USA. ²Program in Atmospheric and Oceanic Science, Princeton University, Princeton, USA. ³Department of Atmospheric and Oceanic Science, Peking University, Beijing, China. ⁴Department of Civil and Environmental Engineering, Princeton University, Princeton, USA. ✉e-mail: miz@princeton.edu; Mauzerall@princeton.edu

previous research presents inconsistent findings regarding how weather conditions, such as atmospheric stagnation, will change in face of global warming^{19,29–32}. Specifically for northern India, both increasing³⁰ and decreasing^{31,32} occurrences of pollution-favorable patterns are projected by the late 21st century. This discrepancy highlights the challenge in understanding climate change impacts on stagnation and, consequently, air quality in India. In addition, some research utilized stagnation indices initially developed for the US by the National Oceanic and Atmospheric Administration (NOAA)^{29,30}. These indices, however, fail to capture the complex and region-specific meteorological conditions influencing PM_{2.5} levels in northern India^{16,22}.

To address these issues, we develop an India-specific atmospheric stagnation index (India-ASI). Our new index is built upon the observational relationships between surface PM_{2.5} concentrations and meteorological variables, leveraging India's recent expansion of its national air quality continuous monitoring network (Supplementary Fig. 1)³³. The India-ASI effectively links stagnant atmospheric conditions and surface PM_{2.5} increases over India, and thus provides an improvement over the NOAA index. Applying our India-ASI, we evaluate projected changes in stagnation occurrences and subsequent PM_{2.5} changes, using an ensemble of the CMIP6 (Climate Model Intercomparison Project Phase 6) climate simulations. We analyze three global warming scenarios with varying regional aerosol trajectories. We find that as climate warms due to rising CO₂, annual stagnation occurrences decrease across most of India, yet winter stagnation occurrences increase over the Indo-Gangetic Plain (IGP), where half of India's 1.4 billion population resides and where the worst air pollution levels already occur in winter. Furthermore, atmospheric aerosols—mainly from anthropogenic emissions—increase stagnation across all seasons. Our analysis underscores the compound influence of increasing CO₂ levels and aerosol emissions in driving variations in 21st-century stagnation across India. Particularly, we identify that these factors synergistically exacerbate winter stagnation in the IGP, highlighting the urgent need for targeted air quality measures.

Results

Use of an India-specific stagnation index to identify surface PM_{2.5} increases

We formulate the daily binary India-ASI using three meteorological variables: precipitation, 10-m wind speed (WS_{10m}), and temperature inversions between 925hPa and 2 m (T_{925hPa-T2m}) (Methods). These variables were chosen as they exhibit robust associations with elevated PM_{2.5} surface concentrations (Supplementary Figs. 2 and 3), and collectively represent the primary processes impacting stagnation: wet scavenging, horizontal dispersion, and vertical dispersion. Specifically, we find substantial PM_{2.5} increases on dry days (precipitation ≤1 mm) compared to precipitation days. In addition, we observe a combined effect of temperature inversions and surface winds on normalized PM_{2.5} levels on dry days (Fig. 1). Figure 1, synthesized by aggregating data from various regions of India, represents a spatially averaged relationship between T_{925hPa-T2m}, WS_{10m}, and PM_{2.5} concentrations. We find elevated PM_{2.5} levels in the upper left section of each panel, associated with suppressed dispersion resulting from weak surface winds (low WS_{10m} values) and strong inversions (high T_{925hPa-T2m} values). The black lines, fitted using 100% normalized daily PM_{2.5} levels, represent the average dispersion conditions associated with the average seasonal PM_{2.5} concentrations on dry days. Thus, our India-ASI defines a stagnation day when the following conditions are fulfilled: (1) daily precipitation ≤1 mm (dry day), and (2) daily WS_{10m} and T_{925hPa-T2m} falling above the black lines in Fig. 1 (weak dispersion day).

Applying the India-ASI, we explore the occurrence and distribution of stagnation across India (Fig. 2a). Stagnation is prevalent in inland regions across India particularly in the north. Specifically, annual stagnation occurrences are -101 ± 57 days (-28% ± 16%) in the

IGP, the most polluted region in the country. In contrast, annual stagnation days are only 43 ± 41 days (-12% ± 11%) in the states south of 18° N. Notably, the IGP also experiences high stagnation persistence, with each stagnation event typically lasting between -2 ± 1 (monsoon) to -4 ± 3 (post-monsoon) consecutive days across seasons. Further examination reveals that northern India (including the IGP) experiences weaker surface winds, stronger temperature inversions, and less frequent precipitation (Supplementary Fig. 4), resulting in more stagnation occurrences and longer durations of consecutive stagnation days compared to southern India. Given the widespread distribution of stagnation across India as identified by the India-ASI, we further investigate the spatial distribution of PM_{2.5} increases during stagnation periods.

The India-ASI effectively predicts PM_{2.5} increases in various regions of India (Fig. 2b), despite the fact that the division between stagnation and non-stagnation days is based on spatially aggregated data from all regions (Fig. 1). In -90% of areas that have PM_{2.5} measurement sites, seasonal PM_{2.5} levels are higher on stagnation days than non-stagnation days. This effect is most evident during winter in the IGP, where PM_{2.5} concentrations increase by -45 ± 20 μg/m³ (-45% ± 13%) during stagnation days. In Central India, despite higher occurrences of stagnation compared to the IGP, the stagnation-induced increases in PM_{2.5} are lower due to the region's significantly lower emission intensities. A few areas experience slightly higher seasonal PM_{2.5} levels on non-stagnation days, possibly due to strong winds carrying pollutants from distant regions. Nevertheless, on an annual basis, all analyzed areas experience PM_{2.5} increases on stagnation days compared to non-stagnation days: -27 ± 10 μg/m³ (-34% ± 8%) in the IGP and -10 ± 7 μg/m³ (-24% ± 13%) across other areas of India. This demonstrates the capability of our index to predict PM_{2.5} increases across India.

We find significant correlations between monthly and regional mean stagnation occurrences (calculated by the India-ASI) and PM_{2.5} concentrations, both in the IGP and across all of India (Table 1 and Supplementary Fig. 5). The Pearson correlation coefficients range from 0.63 ($p = 0.03$, winter) to 0.84 ($p < 0.01$, monsoon) in the IGP, and from 0.66 ($p = 0.01$, pre-monsoon) to 0.84 ($p < 0.01$, winter) in India. This underscores the consistency of the relationship between stagnation occurrences and PM_{2.5} concentrations over the analyzed period of Dec 2017 to May 2022.

Comparison of the India-ASI with the NOAA stagnation index

To illustrate the advancements introduced by the India-ASI, we compare it with the NOAA stagnation index, which was developed for the US and has been previously applied to India^{16,30}. One fundamental difference between our index and the NOAA index lies in the variables chosen to represent near-surface vertical dispersion strength (Methods). While our index uses T_{925hPa-T2m}, the NOAA index primarily relies on mid-tropospheric wind speed (WS_{500hPa})²⁴.

T_{925hPa-T2m} and WS_{500hPa} exhibit marked differences in their association with elevated surface PM_{2.5} across India. We observe significant surface PM_{2.5} increases across locations and seasons when there are strong inversions (high T_{925hPa-T2m} values) indicative of weakened dispersion (Supplementary Fig. 3b). In comparison, during periods of low WS_{500hPa} when weak dispersion is expected by the NOAA index, we observe much weaker surface PM_{2.5} increases or even PM_{2.5} decreases (Supplementary Fig. 3a), which is also found by a previous study¹⁶. This stems from the weak lower-tropospheric wind shear prevalent over northern India, which hinders the downward transport of momentum associated with mid-tropospheric winds²². This weak wind shear results in a decoupling between the surface layer and the mid-troposphere, leading to strong mid-tropospheric winds alongside weak surface winds, especially in winter (Supplementary Fig. 4). Therefore, WS_{500hPa} is less indicative of near-surface stagnation over northern India, compared with T_{925hPa-T2m}.

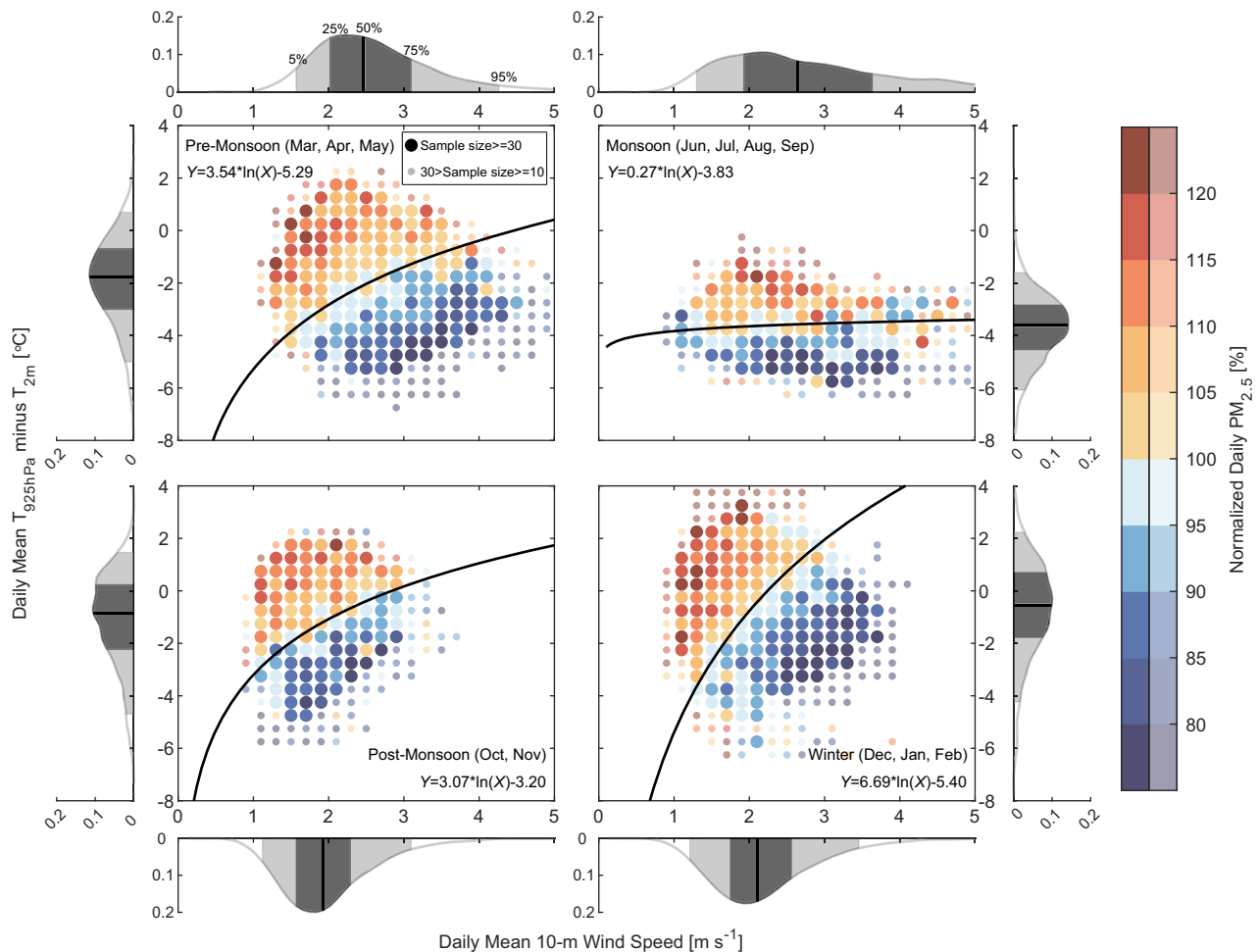


Fig. 1 | Seasonal dependence of normalized daily $PM_{2.5}$ on meteorological conditions across India. We aggregate $PM_{2.5}$ and meteorological data from 116 $PM_{2.5}$ measurement sites across India from Dec 2017 to May 2022 (see their locations in Supplementary Fig. 1a). We focus exclusively on dry days and normalized daily mean $PM_{2.5}$ concentrations by station, season, and year (Methods). The black lines are fitted to 100% normalized daily $PM_{2.5}$ levels (only dots with over 30 samples are used for fitting), indicating the average dispersion conditions during dry

days in each season. Areas above (below) the black lines are defined as weak (strong) dispersion days that are associated with elevated (reduced) $PM_{2.5}$ levels. The outer panels show the frequency distribution of daily meteorological conditions across $PM_{2.5}$ measurement sites during dry days for each season (see top left for frequency labels). Light gray and dark gray shadings indicate the range from the 5th to the 95th percentile and the interquartile range (i.e., 25th to 75th percentile), respectively. The black lines mark the median values.

The NOAA index's dependence on WS_{500hPa} limits its ability to predict $PM_{2.5}$ increases particularly over northern India. When applying the NOAA index, we find that stagnation is almost absent (-13 ± 15 days, or $-14 \pm 17\%$) in the IGP during winters when $PM_{2.5}$ pollution is at its worst (Supplementary Fig. 6). In addition, stagnation occurrences exhibit almost no correlation (e.g., $R = -0.14$, $p = 0.67$) with regional $PM_{2.5}$ levels during winters in the IGP (Table 1 and Supplementary Fig. 5). In comparison, the India-ASI consistently shows positive correlations between monthly $PM_{2.5}$ and stagnation occurrences across seasons ($R \geq 0.63$, $p \leq 0.08$). Consequently, the India-ASI estimates higher annual $PM_{2.5}$ increases ($-17 \pm 12 \mu\text{g}/\text{m}^3$) on stagnation days across India, compared with the NOAA index ($-5 \pm 5 \mu\text{g}/\text{m}^3$). Given the advancements provided by the India-ASI, we apply this region-specific index in subsequent sections.

Changes in stagnation occurrences during the 21st century

Building on the revealed linkage between surface $PM_{2.5}$ pollution and stagnation occurrences identified by the India-ASI, we now focus on future stagnation projections during the 21st century. We utilize two future high-warming scenarios, SSP370 and SSP585, and compare their results with results from twenty years of the historical scenario (1995–2014). While both SSP scenarios include substantial increases in

the global mean temperature, they have very different assumptions on regional energy and air quality policies. Specifically, SSP585 projects an energy transition from coal to natural gas and strong end-of-pipe air pollution controls, resulting in an overall decreasing trend of aerosols and their precursor emissions. In contrast, SSP370 projects continued coal dependence and limited air pollution controls, resulting in much higher air pollutant emissions compared with SSP585 (Supplementary Fig. 7)³⁴.

In projections for the late-21st century (2080–2099), changes in stagnation occurrences exhibit some similarities across the two SSP scenarios. Under the SSP585 scenario, we project decreases in annual stagnation occurrences by -21 ± 13 days across India, compared to the historical period (1995–2014) (Fig. 3a). Stagnation occurrences will decrease in all seasons except winter, and the most pronounced reduction will occur during the monsoon season by -11 ± 5 days (Fig. 3b). However, marginal increases in stagnation occurrences are projected in winter in the IGP under SSP585. Similarly, under the SSP370 scenario, the majority of the country will experience decreases in annual stagnation days, leading to a national average reduction of -10 ± 9 days (Fig. 3c). In addition, similar to SSP585, SSP370 is projected to experience a notable decrease in stagnation days during the monsoon season (Fig. 3d). However, during winters, we project a more

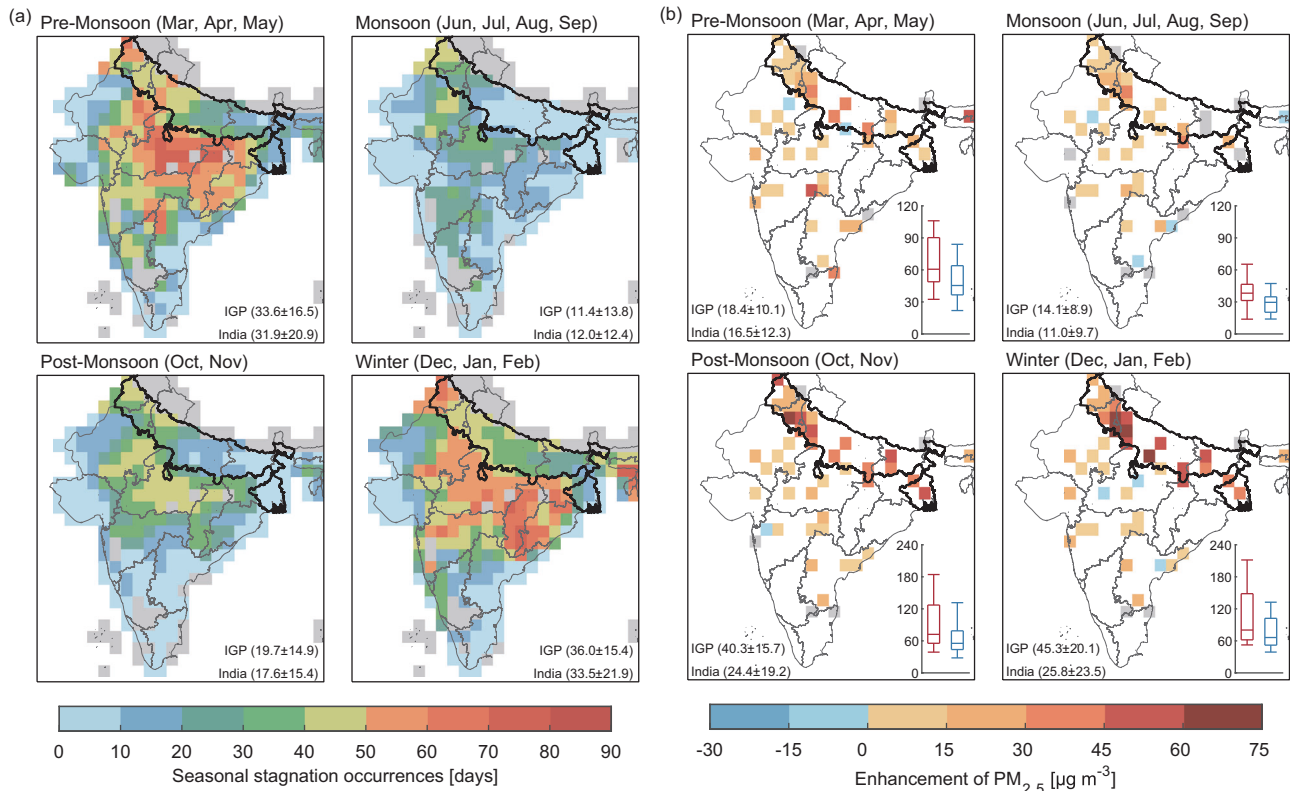


Fig. 2 | Stagnation occurrence and its impact on surface $PM_{2.5}$. Spatial distribution of (a) stagnation occurrences and (b) surface $PM_{2.5}$ increases on stagnation days compared to non-stagnation days over India from Dec 2017 to May 2022. We use the India-ASI to calculate stagnation occurrences and $PM_{2.5}$ increases (Methods). Gray areas indicate regions where stagnation is absent throughout the season or temperatures at the 925 hPa layer are unavailable for stagnation estimation. In **a** and **b**, inset numbers represent the mean \pm one standard deviation, calculated across all available data points within each region: the Indo-Gangetic

Plain (IGP, bounded by thick black lines) or the studied region referred to as India (see geographic range in Supplementary Fig. 1a). In **b**, inset box-whisker plots demonstrate the distribution of seasonal mean $PM_{2.5}$ concentrations on stagnation days (in red) and non-stagnation days (in blue) across all areas with available $PM_{2.5}$ measurements in India. The boxes denote the 25th, 50th, and 75th percentiles, and the whiskers denote the 5th and 95th percentiles of $PM_{2.5}$ concentrations across areas with $PM_{2.5}$ measurement sites in India.

Table.1 | Correlations^a between monthly mean $PM_{2.5}$ concentrations and stagnation occurrence

India Atmospheric Stagnation Index (India-ASI)				
	Pre-Monsoon	Monsoon	Post-Monsoon	Winter
IGP	R = 0.68 ($p = 0.02$)	R = 0.84 ($p < 0.01$)	R = 0.65 ($p = 0.08$)	R = 0.63 ($p = 0.03$)
India	R = 0.66 ($p = 0.01$)	R = 0.79 ($p < 0.01$)	R = 0.77 ($p = 0.03$)	R = 0.84 ($p < 0.01$)
NOAA Atmospheric Stagnation Index				
	Pre-Monsoon	Monsoon	Post-Monsoon	Winter
IGP	R = 0.21 ($p = 0.50$)	R = 0.73 ($p < 0.01$)	R = -0.78 ($p = 0.02$)	R = -0.14 ($p = 0.67$)
India	R = 0.20 ($p = 0.52$)	R = 0.50 ($p = 0.05$)	R = -0.77 ($p = 0.03$)	R = 0.16 ($p = 0.58$)

^aWe perform linear regression to evaluate the Pearson correlation coefficients (R), and use a t-test to estimate p-values (p) over the Indo-Gangetic Plain (IGP) and all of India. See scatterplots, regression lines, and regression slopes in Supplementary Fig. 5.

widespread and more significant increase in stagnation occurrences over India under SSP370 than under SSP585. Specifically, winter stagnation days are forecast to increase by -7 ± 3 days over the IGP under SSP370. Overall, under both SSP scenarios, our projections indicate a decrease in annual stagnation days across most of India, yet an increase in winter stagnation days in the IGP.

The increases in stagnation days during winters and decreases in other seasons (especially in the monsoon season) arise from inter-

seasonal differences in meteorological drivers during the late-21st century. The significant reduction in stagnation days during the monsoon season, as projected under both SSP scenarios, primarily results from increased precipitation and the weakening of temperature inversions (Supplementary Fig. 8). These meteorological changes subsequently lead to reductions in both dry days and weak dispersion days, which together result in fewer stagnation days (Fig. 3b). In contrast, during winters, climate-induced reductions in surface wind speed are significant in the IGP (Supplementary Fig. 8), contributing to an increase in weak dispersion days—and thus more stagnation days—under both SSP scenarios. In addition, a robust strengthening of temperature inversions is projected in the IGP under the SSP370 scenario, further increasing stagnation occurrences.

In projections spanning the 21st century (2015-2099), annual stagnation occurrences over India are projected to slightly increase till 2020 s (for SSP585) and till 2030 s (for SSP370), followed by a nearly linear decrease as global mean near-surface temperatures increase towards the century's end under both SSP scenarios (Fig. 4a). This annual pattern is accompanied by decreasing seasonal stagnation trends, particularly during the monsoon season across India, and contrasting increasing trends during winters in the IGP (Fig. 4b).

Role of CO_2 increases in driving future stagnation occurrences
These projected stagnation trends (annual decrease across India and winter increase in the IGP) in the two SSP scenarios are reproduced in a CO_2 -induced global warming scenario (Figs. 4a, b and 5), indicating the role of CO_2 on future stagnation patterns. Specifically, under CO_2

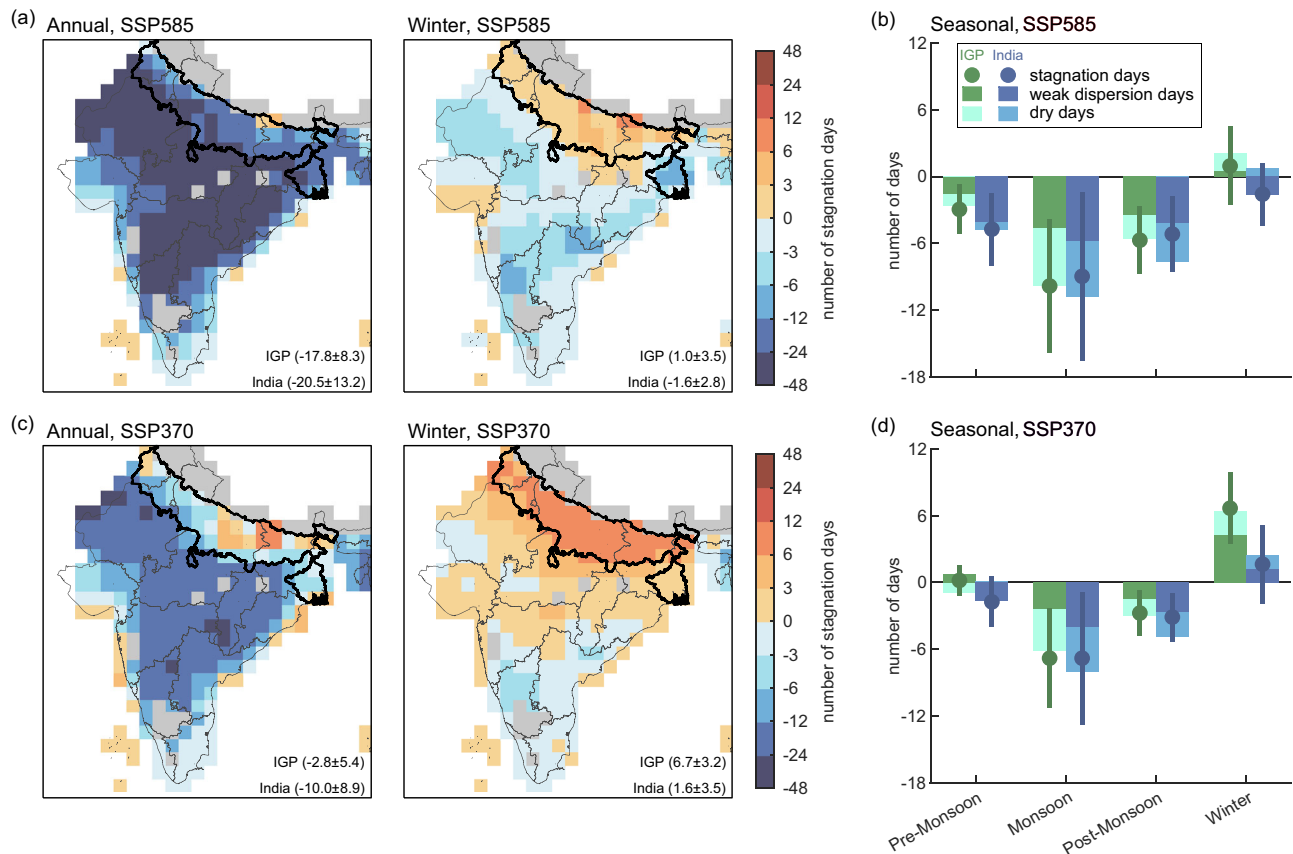


Fig. 3 | Changes in stagnation occurrences simulated using SSP585 and SSP370 during the late 21st century (2080–2099), compared with the historical period (1995–2014). Spatial distribution of multi-model averaged changes in annual and winter stagnation days in (a) SSP585 and (c) SSP370. Inset numbers represent the multi-model mean change \pm one standard deviation in the number of regional mean stagnation days for the Indo-Gangetic Plain (IGP, bounded by thick black

lines) or India (see geographic range in Supplementary Fig. 1a). Gray indicates areas where temperatures at the 925 hPa layer are unavailable. **b, d** Regional mean changes \pm one standard deviation in seasonal stagnation days over the IGP (as green dots and lines) or India (as blue dots and lines) in (b) SSP585 and (d) SSP370. Bars indicate the changes in number of dry days (daily precipitation ≤ 1 mm) and weak dispersion days (defined in Fig. 1).

warming, we project increasingly more precipitation (fewer dry days) and weaker temperature inversions (fewer weak dispersion days) during the monsoon season as climate warms (Supplementary Fig. 9). This results in a national average reduction of stagnation occurrences by -2 ± 1 per 1°C of global warming during the monsoon season over India, which increases the removal and dispersion of air pollutants. In contrast, during winter, warming-induced changes in temperature inversions are minimal over most areas in India, while reductions in both precipitation days (more dry days) and surface wind speed (more weak dispersion days) are evident in the IGP, leading to -1 ± 1 more winter stagnation day per 1°C of global warming. These patterns suggest that global warming might generally improve air quality across India, with the exception of the winter season in IGP. Supporting these findings, a prior study that focused on annual mean conditions also found that CO_2 -driven global warming increases vertical mixing over India, which they suggest may lead to improved air quality³⁵.

Under CO_2 warming, differences in seasonal changes in meteorological conditions over India largely stem from an increased land-ocean thermal contrast. This contrast is enhanced by the fact that the air above tropical lands warm more than the air above oceans primarily because oceans have a larger source of moisture which, when evaporated, restrain warming due to latent heat absorption during evaporation^{36,37}. Consequently, the enhanced temperature contrast between land and ocean induces anomalies in the sea level pressure (SLP) gradient. This altered SLP gradient leads to moisture convergence over land, which in turn boosts monsoon precipitation and delays its retreat over India^{38–41}. This results in more precipitation and fewer dry days during the

monsoon and post-monsoon seasons, favoring wet removal of air pollutants. However, the situation in the IGP during winter is different. There, changes in temperature inversions are minor, while the anomalous southeastern wind significantly weakens the prevailing wind at the surface during winter, increasing winter stagnation occurrences. Beyond the SLP-induced changes, both the frequency and intensity of western disturbances—synoptic systems crucial for winter precipitation—are projected to decline with global warming, which reduces winter rainfall and simultaneously leads to weaker surface winds over the IGP^{19,42}. These CO_2 -induced circulation changes under global warming contribute to the stagnation trends we project for the two SSP scenarios, particularly during the second half of the 21st century.

Role of aerosols in driving future stagnation occurrences

However, despite similarities discussed, there are notable differences in stagnation projections between the two SSP scenarios. Specifically, throughout the 21st century, when equivalent global warming levels for the two scenarios are compared, we consistently project higher annual stagnation occurrences under SSP370 than under SSP585 (Fig. 4a, see seasonal comparisons in Supplementary Fig. 10). Disparities in annual stagnation occurrence between the two SSP scenarios are primarily attributed to their differences in temperature inversions at equivalent global warming levels (Fig. 4c, see other meteorological conditions in Supplementary Fig. 11).

Elevated near-surface aerosol concentrations significantly enhance lower tropospheric temperature inversions (Fig. 4d), leading to more favorable conditions for atmospheric stagnation. The differences

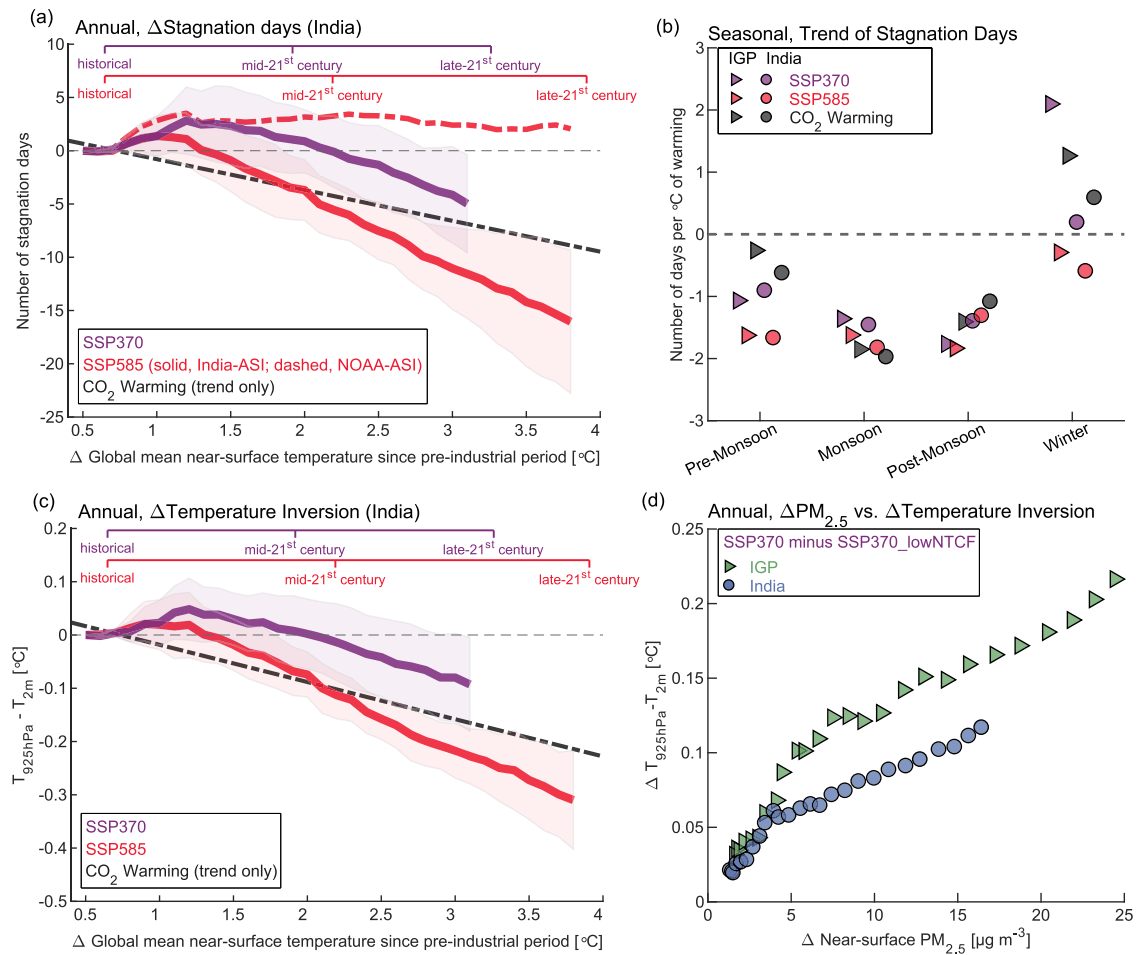


Fig. 4 | Responses of stagnation occurrences and temperature inversions to climate warming and varying regional aerosol concentrations. **a, c** Multi-model twenty-year mean changes (lines) in annual and regional average of (a) stagnation occurrences and (c) temperature inversions over India, compared with the historical period (1995–2014). Both are shown as a function of increases in the global mean temperature since the pre-industrial period (lower x-axis). Shadings represent mean \pm one standard deviation. Results are aggregated into 0.1 $^{\circ}$ C temperature intervals and only presented for intervals with data available for more than 75% of the CMIP6 models. The upper x-axes denote the multi-model median levels of global warming in the historical period, the mid-21st century (2040–2059), and the late-21st century (2080–2099) in SSP585 and SSP370. **b** Linear trends of multi-

model mean stagnation days from 2015 to 2099 for two SSP scenarios and over the 150-year span of the CO₂ warming scenario, in the Indo-Gangetic Plain (IGP, triangles) or India (circles). In **a–c**, CO₂ warming results are from an idealized CO₂-induced global warming scenario, where CO₂ concentrations rise from pre-industrial levels to \sim 1200 ppm over the 150-year period (Methods). **d** Impact of elevated aerosol concentrations on temperature inversions averaged every 20 years from 2015 to 2054 in the IGP (triangles) or India (circles). In **d**, results are from the difference between the SSP370 scenario and the SSP370 scenario with low near-term climate forcers including aerosols (SSP370_lowNTCF, Methods). See the emission trajectories for SSP370, SSP370_lowNTCF, and SSP585 in Supplementary Fig. 7.

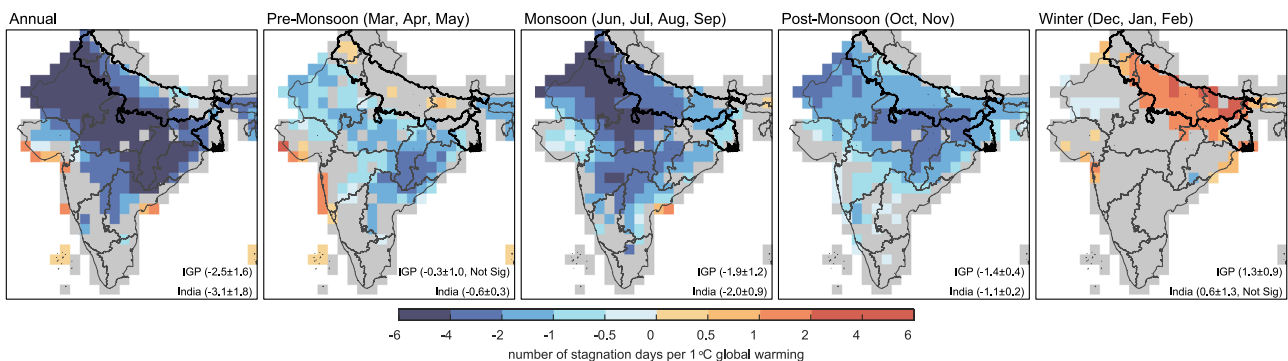


Fig. 5 | Trends in stagnation occurrences against the global mean near-surface temperature increases under CO₂ warming. We show the spatial pattern of multi-model averaged trends in the number of annual and seasonal stagnation days per 1 $^{\circ}$ C of global warming. We perform t-tests to assess the significance of the slope for each CMIP6 model, using a cutoff threshold *p*-value of 0.01. Gray indicates areas where temperatures at the 925 hPa layer are unavailable, or where the slopes are

insignificant across models (i.e., less than 75% of model slopes have the same sign of change as the mean slope). Inset numbers represent the multi-model mean trend \pm one standard deviation for the regional mean stagnation occurrence for the Indo-Gangetic Plain (IGP, bounded by thick black lines) or India (see geographic range in Supplementary Fig. 1a). Numbers followed by ‘Not Sig’ indicate that the regional mean trend is insignificant across models.

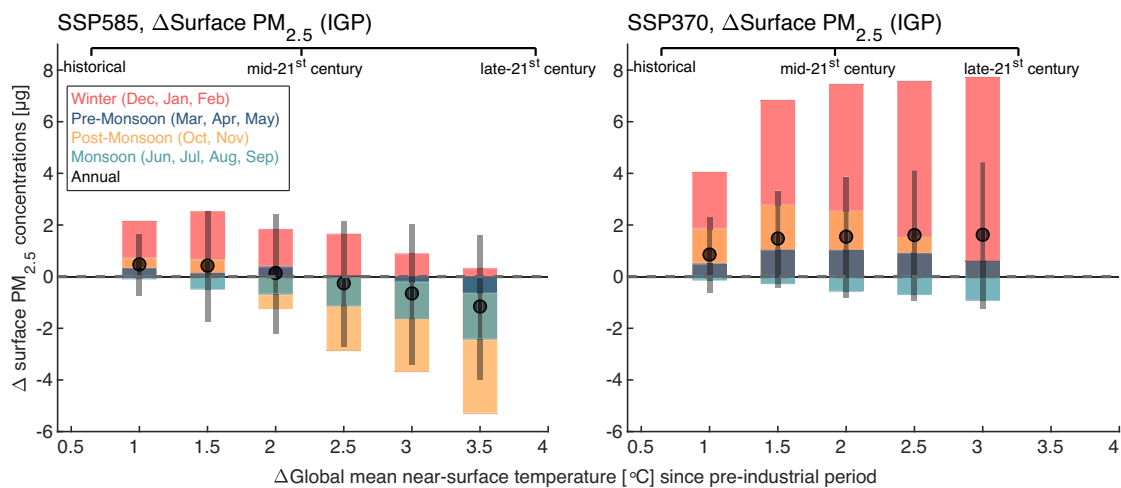


Fig. 6 | Changes in surface $PM_{2.5}$ concentrations due to climate-induced changes in stagnation in the Indo-Gangetic Plain (IGP) during the 21st century. The black dots and colored shadings illustrate the 20-year annual and seasonal average changes in $PM_{2.5}$ concentrations in the IGP, respectively, compared with the historical period (1995–2014). The gray lines represent the mean \pm one standard deviation of the annual $PM_{2.5}$ changes across the CMIP6 models. Results are shown

at each 0.5 °C global warming interval and only presented for intervals with data available for more than 75% of the CMIP6 models. Results only account for areas with available $PM_{2.5}$ measurement sites in the IGP (see their locations in Fig. 2b or Supplementary Fig. 1a). The upper X-axes denote the multi-model median levels of global warming in the historical period, the mid-21st century (2040–2059), and the late-21st century (2080–2099) in SSP585 and SSP370.

between SSP370 and SSP370 with low near-term climate forcers including aerosols (SSP370_lowNTCF) reveal the causal impact of increases in surface $PM_{2.5}$ concentrations on enhancements in temperature inversions. This occurs because atmospheric aerosols, including $PM_{2.5}$, perturb downward shortwave radiation^{43–45}, leading to atmospheric heating (in the presence of black carbon aerosols) and near-surface cooling effects. An aerosol measurement campaign in the northern Indian Ocean supports this and demonstrated that black carbon aerosols significantly enhance inversions and suppress mixing within the boundary layer⁴⁶. Because the SSP370_lowNTCF scenario did not archive sufficient daily meteorological data for our further analysis, we then compare SSP370, with high aerosols, to SSP585, with low aerosols, at the same levels of global warming to demonstrate the role of aerosols on stagnation occurrences. We find SSP370 projects stronger temperature inversions and, thus, more frequent stagnation occurrences relative to SSP585 throughout the 21st century. This underscores how aerosols enhance meteorological conditions conducive to pollution accumulation, which will in turn increase surface $PM_{2.5}$ concentrations⁴⁷.

Compound role of CO₂ and aerosols in driving future stagnation occurrences

Projected trajectories in 21st-century stagnation occurrences across India are influenced by the interplay between global warming—primarily driven by rising CO₂ concentrations—and local meteorological responses to changing aerosol emissions. Under the SSP370 scenario, annual average aerosol concentrations are projected to increase after 2015, followed by a slow decrease after the 2050 s. However, aerosol concentrations in SSP370 are above the historical average (1995–2014) throughout 2015–2099, due to persistently high emissions of aerosol precursors (e.g., ammonia and nitrogen oxides in Supplementary Fig. 7). In contrast, under the SSP585 scenario, annual average aerosol concentrations will slightly increase after 2015, followed by a rapid decline after the 2030 s, with end-of-century concentrations falling below historical levels. Consequently, from 2015 to the 2050 s in SSP370 (and from 2015 to the 2030 s in SSP585), global warming will reduce stagnation occurrences across India, while increasing aerosol concentrations will have the opposite effect. After the 2050 s in SSP370 (and the 2030 s in SSP585), the combined effects of global warming and decreasing aerosol concentrations are projected to drive a pronounced decreasing trend (noted as days per °C of global warming) in annual stagnation

occurrences across India, surpassing the trend projected under a scenario of CO₂-induced warming alone (Fig. 4a, where the slopes of two SSPs are steeper than the slope of CO₂ warming in the second half of the 21st century).

Despite the national trend towards an end-of-century reduction in annual stagnation, winter stagnation occurrences in the IGP are projected to increase throughout the 21st century, compared with the historical period (Supplementary Fig. 10). Specifically, under the SSP370 scenario, the IGP's sustained high aerosol levels are projected to intensify global warming-induced increases in winter stagnation, resulting in regional mean increases of -5 ± 2 and -7 ± 3 stagnation days/winter during 2040–2059 and 2080–2099, respectively. In contrast, the SSP585 scenario predicts aerosol concentrations increasing until the 2030s and falling to below historical levels during 2080–2099. These changes in aerosol concentrations, combined with global warming, lead to increases in stagnation occurrences in the IGP by -2 ± 3 days/winter for the 2030 s and -1 ± 3 days/winter during 2080–2099 under SSP585, compared with the historical period.

Impact of climate-induced stagnation changes on surface $PM_{2.5}$ concentrations

We estimate the response in surface $PM_{2.5}$ concentrations to changes in future stagnation occurrences over the IGP during the 21st century (Methods). In the high-aerosol scenario (SSP370), winter increases in $PM_{2.5}$ concentrations over the IGP can reach up to $-7 \mu\text{g}/\text{m}^3$ if global mean temperature rises above 3 °C towards the late-21st century (Fig. 6). These persistent winter $PM_{2.5}$ increases, driven by more frequent pollution-trapping stagnation, pose a challenge to policy efforts aimed at improving air quality. However, the annual net changes in stagnation-induced $PM_{2.5}$ enhancements are smaller than during winters, due to seasonal variations. For SSP585 in the IGP, the marginal increase in winter $PM_{2.5}$ concentrations are counterbalanced by substantial reductions in other seasons, leading to annual decreases in $PM_{2.5}$ concentrations for most of the 21st century. In contrast, in the SSP370 scenario, the substantial winter increases in $PM_{2.5}$ are not sufficiently offset by decreases in other seasons, resulting in annual stagnation-induced $PM_{2.5}$ enhancements that remain consistently above historical levels throughout the 21st century. A comparison between the two scenarios, at equivalent global warming levels, illustrates a win-win opportunity existing in a low-pollution

future, where strong pollution controls not only directly improve air quality, but also reduce stagnation occurrences and lead to further reductions in surface PM_{2.5} concentrations.

Discussion

Atmospheric stagnation significantly exacerbates surface PM_{2.5} pollution, and thus understanding its response to climate change is crucial for effective future air quality management. In this study, we develop a region-specific stagnation index for India that effectively links stagnant atmospheric conditions and surface PM_{2.5} increases. This index provides a robust tool to understand the impact of climate change on air quality via altering pollution-favorable conditions. Projections for the 21st century indicate that, compared with the historical period of 1995–2014, annual stagnation occurrences will decrease across most of India, while winter stagnation occurrences will increase in the IGP—the most polluted and most populated region in India. Our findings indicate that the projected changes in stagnation are predominantly driven by the compound effects of CO₂-induced global warming and regional meteorology perturbed by aerosols. We find these factors synergistically intensify stagnation in winter over the IGP, leading to increases in stagnation occurrences by -7 days each winter during the late-21st century (2080–2099) in the high-warming and high-aerosol SSP370 scenario.

To better inform air quality policies, the accuracy of projections is important. Our analysis reveals significant differences between projections made by our newly developed India-ASI index and those using the existing NOAA index. Specifically, under the SSP585 scenario, our index predicts a decrease in annual stagnation occurrences across India by -22 days and in the IGP by -18 days during 2080–2099. In contrast, the NOAA index forecasts an annual increase of -2 days for India (Fig. 4a) and -12 days for the IGP over the same period (see spatial differences of the two projections in Supplementary Fig. 12). This discrepancy is notable, especially since one previous study employing the NOAA index under the high-warming RCP8.5 scenario projected even larger end-of-century increases in stagnation occurrences than our projection using the NOAA index³⁰. The NOAA index's projections of increasing annual stagnation occurrences largely result from the expected weakening of mid-tropospheric winds (a key component of this index) over northern India, including the IGP, as a result of a weakening Hadley Circulation under global warming⁴⁸. However, given the decoupling between the mid-troposphere and lower-troposphere over northern India, the NOAA index does not consistently capture near-surface PM_{2.5} increases in the region (Supplementary Fig. 6). This shortcoming makes it difficult to use NOAA index-based stagnation projections to infer changes in surface air quality. This underscores the importance of developing and using region-specific statistical methods to understand the impact of climate change on conditions conducive to pollution, and subsequently, on surface air quality.

The CMIP6 model results we used as input to our India-ASI do not provide consistent results on the direction of the change in regional mean winter stagnation in the IGP by the century's end under SSP585, despite the fact that both mean and median projections across CMIP6 models indicate an increase in winter stagnation days from the historical period. Similarly, a previous study focusing on Delhi (located in the IGP) found a mean reduction of pollution-favorable circulation occurrences by 2 days each winter for 2070–2099 under SSP585, yet with significant cross-model variation ranging from -9 to +7 days³¹. These results highlight the inherent uncertainty in predicting end-of-century pollution-favorable condition changes under SSP585 in the IGP during winters, likely resulting from the compensation effects between aerosols and CO₂. Decreasing aerosols will reduce pollution-trapping inversions, while increasing CO₂ will lead to weaker surface wind and less precipitation that both exacerbate pollution. Despite these uncertainties, all models consistently predict that, on average, SSP585 will experience fewer stagnation days, and therefore fewer stagnation-

induced PM_{2.5} concentrations, compared to SSP370 at equivalent levels of global warming throughout the 21st century.

Our results are subject to several limitations and uncertainties. First, we define stagnation days by atmospheric conditions on dry days that are expected to result in higher-than-seasonal-mean PM_{2.5} concentrations. Although we find elevated PM_{2.5} concentrations during stagnation days using observations averaged across multiple years, PM_{2.5} concentrations on a specific stagnation day may not be higher than on a non-stagnation day. Second, our stagnation index is treated as Boolean throughout our analysis, following previous studies^{22,25}. This treatment limits our application of the index to explain PM_{2.5} variability at individual sites. However, there is a gradation in wind speed and inversion parameters, as shown in Fig. 1, leading to varying normalized PM_{2.5} levels. This indicates that our index, constructed using wind speed and inversion strength, can be continuously interpreted to reflect the capacity of atmospheric dispersion to influence PM_{2.5} concentrations on days without precipitation. Third, our projected future changes in PM_{2.5} only account for the dynamic impact of climate change on surface PM_{2.5} concentrations through the modulation of stagnation occurrences. Global warming can also alter PM_{2.5} levels via feedbacks from the biosphere (e.g., increases in biogenic precursor emissions and wildfire-induced emissions) and secondary aerosol formation (e.g., increases in oxidation rates and aerosol volatility)^{15,49–51}. While the inclusion of these processes is beyond the scope of our study, their combined influence with stagnation on PM_{2.5} projections warrants investigation in future studies.

Given the projection that stagnation will increase during winters over the IGP, compared to a significant decrease in other seasons, wintertime air quality interventions in the IGP will become increasingly important as climate warms. Recently, the Graded Response Action Plan (GRAP) was introduced in Delhi to address the escalating air pollution levels during winter. This plan includes a set of actions triggered based on the severity of air pollution. The plan regulates highly polluting industries, controls construction dust, manages private vehicle usage, and restricts the entry of trucks into Delhi. However, while GRAP helps mitigate immediate pollution episodes, it can disrupt economic activities and is not sufficient to address long-term air quality issues. A clean energy transition over India, combined with strong air pollution control measures, will directly improve regional air quality and public health. Since 2019, the Indian government has initiated the National Clean Air Programme (NCAP)⁵², a critical step to mitigate the country's severe PM_{2.5} pollution by targeting emission sources. The insights derived from comparing the two SSP scenarios suggest that stringent air quality policies like the NCAP will not only directly mitigate air pollution, but will also reduce stagnation occurrences as climate warms, thereby yielding additional air quality improvements.

Methods

Surface PM_{2.5} observations and meteorological data

We obtain surface PM_{2.5} measurements from the Central Pollution Control Board (CPCB) Continuous Ambient Air Quality Monitoring network as well as the U.S. Embassy and Consulates air quality monitoring network over India. We retrieve PM_{2.5} data at hourly resolution. We analyze data from December 2017 to May 2022, based on data availability from the CPCB network, which rapidly expanded post-2017³³. We manually screen data availability on the CPCB website and initially select 150 stations (out of 500 stations) that have data available for at least one day each month between December 2017 and May 2022. Next, we apply rigorous quality control measures to calculate daily PM_{2.5} concentrations at each station, following previous studies^{33,53,54} (details can be found in the Supplementary Information). Our study focuses on 116 stations that provide quality controlled daily data for at least 60% of the days within our chosen analysis period. We further check the consistency of the quality-controlled daily PM_{2.5}

concentrations between the Indian CPCB network and the U.S. Embassy and Consulates network in cities where they co-locate. The results reveal high consistency (Pearson correlation coefficient = 0.96) between the PM_{2.5} observations collected by two individual networks, indicating the reliability of our quality-controlled daily PM_{2.5} datasets (Supplementary Fig. 1). Based on their geographic locations, we then aggregate the 116 measurement sites into 46 grid boxes, each with a horizontal resolution of 1° × 1° horizontal resolution.

Furthermore, we use an hourly climate reanalysis dataset (ERAS) from the European Centre for Medium-Range Weather Forecasts (ECMWF), which provides data at a resolution of 0.25° × 0.25°. We calculate daily metrics for each variable and further interpolate the data to match the re-gridded PM_{2.5} data at 1° × 1° horizontal resolution.

Development of the India-specific stagnation index

We develop an improved index to define atmospheric stagnation over India (India-ASI) that builds upon a widely-applied stagnation index by the U.S. National Oceanic and Atmospheric Administration (NOAA)²⁴. The NOAA index identifies stagnation using daily thresholds of three variables: 10-meter wind speed ($WS_{10m} \leq 3.2$ m/s), 500-hPa wind speed ($WS_{500hPa} \leq 13$ m/s), and precipitation ($precip \leq 1$ mm). In addition, when a temperature inversion occurs in the boundary layer, the WS_{10m} criterion is relaxed by 10%. The WS_{10m} influences the strength of atmospheric dispersion, while precipitation controls the washout of local air pollutants. WS_{500hPa} is influenced by the synoptic system; a low WS_{500hPa} indicates a high-pressure system, which is associated with weak vertical dispersion in the U.S..

We conduct both a regression analysis and a composite analysis, performed separately for each season, to investigate relationships between meteorological components of the NOAA index and surface PM_{2.5} concentrations across India (Supplementary Figs. 2 and 3). Prior to performing the regression analysis, we detrend and de-seasonalize the daily meteorological and PM_{2.5} datasets by subtracting the 30-day moving averages from the original time series. This process refines our focus on synoptic-scale variability¹⁴. Our regression analysis calculates the Pearson correlation coefficients between meteorological variables and PM_{2.5} concentrations. In addition, the composite analysis calculates the difference in PM_{2.5} levels between days with high and low anomalies of specific meteorological conditions. Results reveal that the WS_{10m} displays a significant negative correlation ($p < 0.01$) with PM_{2.5} concentrations at ~70% of the measurement stations, while low WS_{10m} anomalies are associated with elevated PM_{2.5} concentrations across most analyzed areas. Similarly, the absence of precipitation considerably increases PM_{2.5} concentrations at over 90% of the analyzed areas across India. However, the WS_{500hPa} exhibits poor correlation with surface PM_{2.5}, showing weak associations at only 9% of the stations during the winter. Consequently, we find a limited association between stagnation days (defined by the NOAA index) and PM_{2.5} increases over India (Supplementary Fig. 6).

To improve the performance of the NOAA index over India, we explore alternatives to the WS_{500hPa} metric. Our objective is to identify a meteorological condition that both statistically and consistently correlates with increases in PM_{2.5}, and physically represents the dynamics of near-surface vertical mixing, thus serving as a replacement for WS_{500hPa} . Specifically, we evaluate the capability of three alternative metrics to predict observed PM_{2.5} increases: temperature inversions between 850 hPa and 2 m ($T_{850hPa-T_{2m}}$), boundary layer height (BLH) and temperature inversions between 925 hPa and 2 m ($T_{925hPa-T_{2m}}$). We select $T_{850hPa-T_{2m}}$ and BLH because they are known to represent vertical mixing and are associated with high PM_{2.5} episodes, particularly during winters in India, as found in previous studies^{16,19,31}. We also include $T_{925hPa-T_{2m}}$ because it represents overall vertical stability for an atmospheric layer that is closer to the surface, making it potentially more relevant for near-surface PM_{2.5} concentrations, compared to the layer represented by $T_{850hPa-T_{2m}}$.

Our results indicate that $T_{925hPa-T_{2m}}$ is the most effective metric that statistically correlates with increases in PM_{2.5}, showing significant correlations at roughly 60–80% of the measurement stations across India (Supplementary Fig. 2b). Additionally, PM_{2.5} levels on days with high $T_{925hPa-T_{2m}}$ anomalies are consistently and notably higher than on days with low anomalies $T_{925hPa-T_{2m}}$ across all seasons (Supplementary Fig. 3b). In contrast, the correlations between PM_{2.5} levels and the other two metrics ($T_{850hPa-T_{2m}}$ and BLH) show inconsistent results across seasons, with particularly weaker significance of seasonal correlations compared to those observed with $T_{925hPa-T_{2m}}$. In addition, we apply radiosonde data collected at Delhi and Kolkata from 2017 to 2022, which reveals a more consistent seasonal dependence of PM_{2.5} levels on $T_{925hPa-T_{2m}}$ compared to $T_{850hPa-T_{2m}}$ and BLH (Supplementary Fig. 13). This further supports our finding that $T_{925hPa-T_{2m}}$ is the most effective metric to predict increases in PM_{2.5}.

In light of these results, we select $T_{925hPa-T_{2m}}$ as the alternative to the WS_{500hPa} metric used in the NOAA index. We continue to use precipitation and WS_{10m} metrics in our index due to their strong association with elevated PM_{2.5} levels across India in all seasons.

We follow the method of Wang²² to define an atmospheric stagnation day over India, which is different from traditional approaches (e.g., setting cut-off values for each meteorological variable). First, we exclude rainy days (days with total precipitation exceeding 1 mm) and focus our study on dry days, which could potentially feature stagnation. Next, we normalize the daily PM_{2.5} concentrations against the seasonal mean PM_{2.5} concentrations for each station, each season, and each year. This step lessens the influence of spatially and seasonally varying emission intensities on observed daily PM_{2.5} levels. Then, we map all normalized daily PM_{2.5} data onto a coordinate system where the X-axis represents daily WS_{10m} and the Y-axis represents daily $T_{925hPa-T_{2m}}$ (Fig. 1). In the coordinate system, results are aggregated by WS_{10m} and $T_{925hPa-T_{2m}}$ intervals of 0.2 m/s and 0.5 °C, respectively, and are shown only when there are at least 10 daily samples in the interval. Finally, we fit the points close to 100% normalized daily PM_{2.5} levels. Points above the fitted curve are indicative of elevated PM_{2.5} levels (i.e., higher than seasonal mean) on dry days with weak atmospheric dispersion. Conversely, points below the curve suggest reduced PM_{2.5} levels on days with stronger dispersion. We define an atmospheric stagnation day if (1) daily precipitation ≤ 1 mm (representing a dry day), and (2) daily WS_{10m} and $T_{925hPa-T_{2m}}$ fall above the black lines in Fig. 1 (representing a weak dispersion day).

Increases in PM_{2.5} concentrations ($\Delta PM_{2.5}$) due to stagnation in a given period are calculated as follows:

$$\Delta PM_{2.5} = PM_{2.5_stag} - PM_{2.5_non-stag}$$

Where $PM_{2.5_stag}$ represents mean PM_{2.5} concentrations during stagnation days in that period, and $PM_{2.5_non-stag}$ represents mean PM_{2.5} concentrations during non-stagnation days in that period.

Estimation of climate-change-driven changes in stagnation occurrences

The projection of future stagnation occurrences fundamentally depends on the prediction of key meteorological variables that define stagnation, such as temperature inversions and precipitations, under future climate conditions. The sensitivity of these variables to global warming and the sensitivity of global warming to anthropogenic forcings are critical factors influencing these predictions. Climate models have a wide spread in simulating these sensitivities due to their structural differences and varying capabilities to simulate aerosol and cloud feedbacks⁵⁵. This leads to divergent projections of future meteorological conditions, even when driven by identical anthropogenic forcings. In our study, we address this issue by utilizing a set of climate models to predict ensemble-mean stagnation changes, following previous research^{19,26,29,30}. This ensemble approach helps

mitigate individual model biases and provides a more robust prediction of future conditions.

We examine the impact of climate change on stagnation using 8 climate models (12 ensembles in total) from the Climate Model Inter-comparison Project Phase 6 (CMIP6, Supplementary Table 1). These models were selected based on their availability of necessary daily meteorological variables (i.e., T_{925hPa} , T_{2m} , WS_{10m} , and precipitation) critical for our analysis, as our index for identifying stagnation events relies on daily resolution data. All model outputs are downloaded from the CMIP6 website (<https://aims2.llnl.gov/search/cmip6/>) and interpolated using a flux-conserved method to align with the $1^\circ \times 1^\circ$ horizontal grid of $PM_{2.5}$ observations and the ERA5 reanalysis.

To analyze stagnation changes throughout the 21st century, we use three CMIP6 scenarios: historical, SSP370, and SSP585. Averages from 1995 to 2014 in the historical scenario set the baseline against which SSP370 and SSP585 projections are compared. Both SSP370 and SSP585 project high global warming by 2100, averaging 3.8 °C and 5.0 °C increases respectively across all CMIP6 models⁵⁶. However, their projections for anthropogenic emissions of air pollutants (including primary aerosols and their gaseous precursors), follow opposite overall trends during the 21st century (Supplementary Fig. 7)⁵⁷. Specifically, in SSP370, anthropogenic primary aerosol emissions (black carbon and organic carbon) are projected to increase until 2050, then decrease by 2100 to slightly below their 2015 levels. For aerosol precursors emissions in SSP370, both NH_3 and NO_x will continuously increase by 2100, while SO_2 will peak by 2050 and then decrease to below their 2015 levels by 2100. In contrast, SSP585 projects substantial and consistent decline in anthropogenic primary aerosol emissions post-2015, with 2100 levels projected to be significantly below those of 2015. For aerosol precursors emissions in SSP585, SO_2 , NO_x and NH_3 , will increase until 2040 and then decline by 2100, with 2100 emissions falling below the 2015 levels. These scenarios facilitate an exploration of future stagnation under varied global warming and air pollution emission trajectories.

To isolate the impact of increasing CO_2 -induced global warming on stagnation occurrences over India, we utilize two CMIP6 benchmark scenarios: piControl and 1pct CO_2 ⁵⁸. The piControl scenario is driven by conditions representative of the pre-industrial period. Conversely, 1pct CO_2 is an idealized climate scenario, where global warming is solely driven by an annual 1% increase in CO_2 concentrations until they quadruple. Over its 150-year simulation, the 1pct CO_2 scenario starts with CO_2 concentrations from the piControl scenario and increases them to ~1200 ppm. The comparison between the 1pct CO_2 and piControl scenarios allows us to directly attribute differences in stagnation patterns across India to the effects of CO_2 -induced global warming.

To contextualize our findings within a range of global warming, and considering the varying climate sensitivities of models, we normalize changes in variables from the 1pct CO_2 (changes relative to piControl), SSP370 (changes relative to historical), and SSP585 (changes relative to historical) scenarios by global mean near-surface temperature increases since the pre-industrial period (calculated using piControl) in each model.

To isolate the causal impact of aerosols on temperature inversions, we examined two distinct sets of climate simulations from AerChemMIP experiments⁵⁹: the SSP370 scenario and the SSP370 scenario with low near-term climate forcings including aerosols. They are identical in all aspects except for the levels of aerosols and their precursor emissions (Supplementary Fig. 7), and are targeted to quantify the impact of short-lived climate forcings on the climate. This controlled setup ensures that any observed differences between these two scenarios in meteorological conditions can be confidently attributed to the effects of aerosols, since all other external forcings, including CO_2 and CH_4 levels, are constant across both scenarios. Given that SSP370_lowNTCF data is only available from 2015 to 2054, we utilize a running 20-year average for this period to facilitate our

scenario comparison. This allows us to attribute any observed differences in meteorological conditions specifically to the influence of aerosols, by contrasting the SSP370 scenario (with its higher aerosol levels), against the SSP370_lowNTCF scenario.

Estimation of stagnation-driven changes in surface $PM_{2.5}$ concentrations

To project the future impact of altered stagnation patterns on surface $PM_{2.5}$ concentrations, we utilize the observed relationship between seasonal mean $PM_{2.5}$ concentrations and stagnation occurrences from December 2017 to May 2022 (Supplementary Fig. 5). We proceed under the assumption that, despite the presence of seasonal variations, the intensity of emissions for a specific season remains relatively consistent across years. We exclude the pre-monsoon season of 2020 when estimating the slope, due to the emission perturbation caused by the pandemics. Therefore, the slopes reflect the dependence of $PM_{2.5}$ on stagnation occurrences. Accordingly, we apply the derived regression slope, which quantifies the rate of change in $PM_{2.5}$ concentrations with respect to changes in stagnation occurrences, to project how future changes in stagnation occurrences, relative to the historical baseline, will influence $PM_{2.5}$ levels.

Data availability

The continuous $PM_{2.5}$ measurement data across India are publicly available and can be retrieved from the Indian CPCB website (<https://airquality.cpcb.gov.in/ccr/#/caaqm-dashboard-all/caaqm-landing>) and the U.S. Embassies and Consulates website (<https://www.airnow.gov/international/us-embassies-and-consulates/>). The hourly climate reanalysis data at the surface level and pressure levels from ERA5 are available at <https://cds.climate.copernicus.eu/#/search?text=ERA5&type=dataset>. The radiosonde data for New Delhi and Kolkata can be accessed from the Integrated Global Radiosonde Archive (IGRA, <https://www.ncei.noaa.gov/products/weather-balloon/integrated-global-radiosonde-archive>). The shapefile for Indian states used in our map plots is provided by GeoBoundaries datasets (<https://www.geoboundaries.org/#tabs1.html>). The CMIP6 model results are publicly available from <https://aims2.llnl.gov/search/cmip6/>. Source data that support all figures in the main text are provided with this paper.

Code availability

The MATLAB modules we developed to load and spatially interpolate the CMIP6 daily and monthly output using a flux-conserved method are provided in Github (<https://github.com/MickeyCKG/Source-Code-For-Indian-Stagnation-Project/releases>). All other custom codes are direct implementation of standard methods and techniques as described in detail in the Methods and Supplementary Information.

References

1. Burnett, R. et al. Global estimates of mortality associated with long-term exposure to outdoor fine particulate matter. *Proc. Natl. Acad. Sci. USA* **115**, 9592–9597 (2018).
2. Collaborators GBDRF. Global burden of 87 risk factors in 204 countries and territories, 1990–2019: a systematic analysis for the Global Burden of Disease Study 2019. *Lancet* **396**, 1223–1249 (2020).
3. McDuffie, E. E. et al. Source sector and fuel contributions to ambient $PM_{2.5}$ and attributable mortality across multiple spatial scales. *Nat. Commun.* **12**, 3594 (2021).
4. Apte, J. S. & Pant, P. Toward cleaner air for a billion Indians. *Proc. Natl. Acad. Sci. USA* **116**, 10614–10616 (2019).
5. India State-Level Disease Burden Initiative Air Pollution C. Health and economic impact of air pollution in the states of India: the Global Burden of Disease Study 2019. *Lancet Planet Health* **5**, e25–e38 (2021).

6. Ravishankara, A. R., David, L. M., Pierce, J. R. & Venkataraman, C. Outdoor air pollution in India is not only an urban problem. *Proc. Natl. Acad. Sci. USA* **117**, 28640–28644 (2020).
7. Peng, W., Kim, S. E., Purohit, P., Urpelainen, J. & Wagner, F. Incorporating political-feasibility concerns into the assessment of India's clean-air policies. *One Earth* **4**, 1163–1174 (2021).
8. Xie, Y., Zhou, M., Hunt, K. M. R. & Mauzerall, D. L. Recent PM_{2.5} air quality improvements in India benefited from meteorological variation. *Nat. Sustain.* **7**, 983–993 (2024).
9. Lelieveld, J., Evans, J. S., Fnais, M., Giannadaki, D. & Pozzer, A. The contribution of outdoor air pollution sources to premature mortality on a global scale. *Nature* **525**, 367–371 (2015).
10. Chowdhury, S. et al. Indian annual ambient air quality standard is achievable by completely mitigating emissions from household sources. *Proc. Natl. Acad. Sci. USA* **116**, 10711–10716 (2019).
11. Cropper, M., et al. The mortality impacts of current and planned coal-fired power plants in India. *Proc. Natl. Acad. Sci. USA* **118**, e2017936118 (2021).
12. Pai, S. J. et al. Compositional Constraints are Vital for Atmospheric PM(2.5) Source Attribution over India. *ACS Earth Space Chem.* **6**, 2432–2445 (2022).
13. Jacob, D. J. & Winner, D. A. Effect of climate change on air quality. *Atmos. Environ.* **43**, 51–63 (2009).
14. Tai, A. P. K., Mickley, L. J. & Jacob, D. J. Correlations between fine particulate matter (PM_{2.5}) and meteorological variables in the United States: Implications for the sensitivity of PM_{2.5} to climate change. *Atmos. Environ.* **44**, 3976–3984 (2010).
15. Shen, L., Mickley, L. J. & Murray, L. T. Influence of 2000–2050 climate change on particulate matter in the United States: results from a new statistical model. *Atmos. Chem. Phys.* **17**, 4355–4367 (2017).
16. Schnell, J. L. et al. Exploring the relationship between surface PM_{2.5} and meteorology in Northern India. *Atmos. Chem. Phys.* **18**, 10157–10175 (2018).
17. Gao, M. et al. Response of winter fine particulate matter concentrations to emission and meteorology changes in North China. *Atmos. Chem. Phys.* **16**, 11837–11851 (2016).
18. Zheng, G. J. et al. Exploring the severe winter haze in Beijing: the impact of synoptic weather, regional transport and heterogeneous reactions. *Atmos. Chem. Phys.* **15**, 2969–2983 (2015).
19. Paulot, F., Naik, V. W. & Horowitz, L. Reduction in Near-Surface Wind Speeds With Increasing CO₂ May Worsen Winter Air Quality in the Indo-Gangetic Plain. *Geophys. Res. Lett.* **49**, e2022GL099039 (2022).
20. Chen, Z. Y. et al. Understanding meteorological influences on PM_{2.5} concentrations across China: a temporal and spatial perspective. *Atmos. Chem. Phys.* **18**, 5343–5358 (2018).
21. Schnell, J. L. & Prather, M. J. Co-occurrence of extremes in surface ozone, particulate matter, and temperature over eastern North America. *Proc. Natl. Acad. Sci. USA* **114**, 2854–2859 (2017).
22. Wang, X., Dickinson, R. E., Su, L., Zhou, C. & Wang, K. PM_{2.5} Pollution in China and How It Has Been Exacerbated by Terrain and Meteorological Conditions. *B Am. Meteorol. Soc.* **99**, 105–119 (2018).
23. Garrido-Perez, J. M., Ordonez, C., Garcia-Herrera, R. & Barriopedro, D. Air stagnation in Europe: Spatiotemporal variability and impact on air quality. *Sci. Total Environ.* **645**, 1238–1252 (2018).
24. Wang, J. X. L. & Angell, J. K. *Air stagnation climatology for the United States (1948–1998)* (NOAA/Air Resource Laboratory ATLAS, 1999).
25. Huang, Q., Cai, X., Wang, J., Song, Y. & Zhu, T. Climatological study of the Boundary-layer air Stagnation Index for China and its relationship with air pollution. *Atmos. Chem. Phys.* **18**, 7573–7593 (2018).
26. Cai, W., Li, K., Liao, H., Wang, H. & Wu, L. Weather conditions conducive to Beijing severe haze more frequent under climate change. *Nat. Clim. Change* **7**, 257–262 (2017).
27. Fiore, A. M. et al. Global air quality and climate. *Chem. Soc. Rev.* **41**, 6663–6683 (2012).
28. Hong, C. et al. Impacts of climate change on future air quality and human health in China. *Proc. Natl. Acad. Sci. USA* **116**, 17193–17200 (2019).
29. Horton, D. E., Harshvardhan & Diffenbaugh, N. S. Response of air stagnation frequency to anthropogenically enhanced radiative forcing. *Environ. Res. Lett.* **7**, 044034 (2012).
30. Horton, D. E., Skinner, C. B., Singh, D. & Diffenbaugh, N. S. Occurrence and persistence of future atmospheric stagnation events. *Nat. Clim. Chang* **4**, 698–703 (2014).
31. Zhang, X. et al. Discordant future climate-driven changes in winter PM_{2.5} pollution across India under a warming climate. *Elem. Sci. Anth.* **11**, 044034 (2023).
32. Li, J. D., Hao, X., Liao, H., Hu, J. L. & Chen, H. S. Meteorological Impact on Winter PM_{2.5} Pollution in Delhi: Present and Future Projection Under a Warming Climate. *Geophys. Res. Lett.* **48**, e2021GL093722 (2021).
33. Sharma, D. & Mauzerall, D. Analysis of Air Quality Data in India between 2015 and 2019. *Aerosol Air Quality Res.*, **22**, 210204 (2022).
34. Gidden, M. J. et al. Global emissions pathways under different socioeconomic scenarios for use in CMIP6: a dataset of harmonized emissions trajectories through the end of the century. *Geosci. Model Dev.* **12**, 1443–1475 (2019).
35. Stjern, C. W., Hodnebrog, O., Myhre, G. & Pisso, I. The turbulent future brings a breath of fresh air. *Nat. Commun.* **14**, 3735 (2023).
36. Byrne, M. P. & O’Gorman, P. A. Trends in continental temperature and humidity directly linked to ocean warming. *Proc. Natl. Acad. Sci. USA* **115**, 4863–4868 (2018).
37. Zhang, Y., Held, I. & Fueglistaler, S. Projections of tropical heat stress constrained by atmospheric dynamics. *Nat. Geosci.* **14**, 133–137 (2021).
38. Turner, A. G. & Annamalai, H. Climate change and the South Asian summer monsoon. *Nat. Clim. Change* **2**, 587–595 (2012).
39. Jin, Q. J. & Wang, C. A revival of Indian summer monsoon rainfall since 2002. *Nat. Clim. Change* **7**, 587–594 (2017).
40. Wang, B., Jin, C. H. & Liu, J. Understanding Future Change of Global Monsoons Projected by CMIP6 Models. *J. Clim.* **33**, 6471–6489 (2020).
41. Fang, C., et al. Impacts of reducing scattering and absorbing aerosols on the temporal extent and intensity of South Asian summer monsoon and East Asian summer monsoon. *Atmos. Chem. Phys.* **23**, 8341–8368 (2023).
42. Hunt, K. M. R., Turner, A. G. & Shaffrey, L. C. Falling Trend of Western Disturbances in Future Climate Simulations. *J. Clim.* **32**, 5037–5051 (2019).
43. Hansen, J., Sato, M. & Ruedy, R. Radiative forcing and climate response. *J. Geophys. Res. Atmos.* **102**, 6831–6864 (1997).
44. Li, Z. Q. et al. Aerosol and boundary-layer interactions and impact on air quality. *Natl. Sci. Rev.* **4**, 810–833 (2017).
45. Andreae, M. O. & Rosenfeld, D. Aerosol–cloud–precipitation interactions. Part 1. The nature and sources of cloud-active aerosols. *Earth Sci. Rev.* **89**, 13–41 (2008).
46. Wilcox, E. M. et al. Black carbon solar absorption suppresses turbulence in the atmospheric boundary layer. *Proc. Natl. Acad. Sci. USA* **113**, 11794–11799 (2016).
47. Zhou, M. et al. The impact of aerosol–radiation interactions on the effectiveness of emission control measures. *Environ. Res. Lett.* **14**, 024002 (2019).
48. Xia, Y., Hu, Y. & Liu, J. Comparison of trends in the Hadley circulation between CMIP6 and CMIP5. *Sci. Bull.* **65**, 1667–1674 (2020).
49. Tai, A. P. K. et al. Meteorological modes of variability for fine particulate matter PM_{2.5} air quality in the United States: implications for PM_{2.5} sensitivity to climate change. *Atmos. Chem. Phys.* **12**, 3131–3145 (2012).

50. Cao, C., et al. Policy-Related Gains in Urban Air Quality May Be Offset by Increased Emissions in a Warming Climate. *Environ. Sci. Technol.* **57**, 9683–9692 (2023).
51. Gomez, J., et al. The projected future degradation in air quality is caused by more abundant natural aerosols in a warmer world. *Commun. Earth Environ.* **4**, 22 (2023).
52. National Clean Air Programme. *Central Pollution Control Board Ministry of Environmental Forests and Climate Change* (TGOI, 2019).
53. Barrero, M. A., Orza, J. A., Cabello, M. & Canton, L. Categorisation of air quality monitoring stations by evaluation of PM(10) variability. *Sci. Total Environ.* **524–525**, 225–236 (2015).
54. Singh, V. et al. Diurnal and temporal changes in air pollution during COVID-19 strict lockdown over different regions of India. *Environ. Pollut.* **266**, 115368 (2020).
55. Wang, C. G., Soden, B. J., Yang, W. C. & Vecchi, G. A. Compensation Between Cloud Feedback and Aerosol-Cloud Interaction in CMIP6 Models. *Geophys. Res. Lett.* **48**, e2020GL091024 (2021).
56. Meinshausen, M. et al. The shared socio-economic pathway (SSP) greenhouse gas concentrations and their extensions to 2500. *Geosci. Model Dev.* **13**, 3571–3605 (2020).
57. Riahi, K. et al. The Shared Socioeconomic Pathways and their energy, land use, and greenhouse gas emissions implications: An overview. *Glob. Environ. Change* **42**, 153–168 (2017).
58. Eyring, V. et al. Overview of the Coupled Model Intercomparison Project Phase 6 (CMIP6) experimental design and organization. *Geosci. Model Dev.* **9**, 1937–1958 (2016).
59. Collins, W. J. et al. AerChemMIP: quantifying the effects of chemistry and aerosols in CMIP6. *Geosci. Model Dev.* **10**, 585–607 (2017).

Acknowledgements

M.Z., Y.-X., and D.L.M. acknowledge support from the M.S. Chadha Center for Global India at Princeton University, the Princeton School of Public and International Affairs and its Center for Policy Research on Energy and the Environment. L.S. acknowledges support from the National Natural Science Foundation of China (42275194) and National Key Research and Development Program of China (2023YFC3707404). We thank Disha Sharma for providing processed CPCB datasets early in this study. We thank Shixian Zhai, Fabien Paulot, Shradda Dhungel, Vaishali Naik, and Larry W. Horowitz for their constructive suggestions. We thank Xinyi Li, Fangxuan Ren, and Qianqian Huang for their help on the interpretation of our results.

Author contributions

M.Z. and D.L.M. conceptualized the study. M.Z. and Y.-Y.X. retrieved the data. M.Z. performed the research. M.Z., D.L.M., and Y.-Y.X.

analyzed the results. C.-G.W. and L.S. helped analyze changing climate dynamics and stagnation-induced PM_{2.5} projections. M.Z. and D.L.M. wrote the manuscript. All authors contributed to the interpretation of findings, provided revisions to the manuscript, and approved the final manuscript.

Competing interests

The authors declare no competing interests.

Additional information

Supplementary information The online version contains supplementary material available at <https://doi.org/10.1038/s41467-024-51462-y>.

Correspondence and requests for materials should be addressed to Mi Zhou or Denise L. Mauzerall.

Peer review information *Nature Communications* thanks Sachchida Tripathi and the other, anonymous, reviewers for their contribution to the peer review of this work. A peer review file is available.

Reprints and permissions information is available at <http://www.nature.com/reprints>

Publisher's note Springer Nature remains neutral with regard to jurisdictional claims in published maps and institutional affiliations.

Open Access This article is licensed under a Creative Commons Attribution-NonCommercial-NoDerivatives 4.0 International License, which permits any non-commercial use, sharing, distribution and reproduction in any medium or format, as long as you give appropriate credit to the original author(s) and the source, provide a link to the Creative Commons licence, and indicate if you modified the licensed material. You do not have permission under this licence to share adapted material derived from this article or parts of it. The images or other third party material in this article are included in the article's Creative Commons licence, unless indicated otherwise in a credit line to the material. If material is not included in the article's Creative Commons licence and your intended use is not permitted by statutory regulation or exceeds the permitted use, you will need to obtain permission directly from the copyright holder. To view a copy of this licence, visit <http://creativecommons.org/licenses/by-nc-nd/4.0/>.

© The Author(s) 2024